

Diffuse X-ray Emission from Late-Type Galaxy Haloes

A. J. Benson^{1,3}, R. G. Bower^{1,4}, C. S. Frenk^{1,5} and S. D. M. White^{2,6}

1. *Physics Department, University of Durham, South Road, Science Laboratories, Durham DH1 3LE, England.*

2. *Max Planck Institute für Astrophysik, Karl-Schwarzschild Strasse 1, D-85740, Garching, Germany.*

3. *E-mail: A.J.Benson@dur.ac.uk*

4. *E-mail: R.G.Bower@dur.ac.uk*

5. *E-mail: C.S.Frenk@dur.ac.uk*

6. *E-mail: swhite@mpa-garching.mpg.de*

31 May 2021

ABSTRACT

Current theories of galaxy formation predict that spiral galaxies are embedded in a reservoir of hot gas. This gas is able to cool onto the galaxy replenishing cold gas that is consumed by star formation. Estimates of the X-ray luminosity emitted in the cooling region suggest a bolometric luminosity of order 10×10^{41} ergs s^{-1} in massive systems. We have used ROSAT PSPC data to search for extended X-ray emission from the haloes of three nearby, massive, late-type galaxies: NGC 2841, NGC 4594 and NGC 5529. We infer 95% upper limits on the bolometric X-ray luminosities of the haloes of NGC 2841, NGC 4594 and NGC 5529 of 0.4, 1.2 and 3.8×10^{41} ergs s^{-1} respectively. Thus, the true luminosity lies well below the straightforward theoretical prediction. We discuss this discrepancy and suggest a number of ways in which the theoretical model might be brought into agreement with the observational results. A possible solution is that the gravitational potentials of these galaxies' dark matter haloes are weaker than assumed in the current model. Alternatively, the present day accretion may be substantially less than is required on average to build the disk over the Hubble time. Our results are, however, based on only three galaxies, none of which is ideal for this kind of study. A larger data set is required to explore this important problem further.

Key words: cooling flows - X-rays: galaxies - galaxies: formation - galaxies: NGC 2841, NGC 4594, NGC 5529

1 INTRODUCTION

In models of galaxy formation by hierarchical clustering, the disks of spiral galaxies form by late accretion of gas which cools from an extended reservoir around the galaxy. In these models disks are still expected to be growing at the present day. Such models have been very successful in accounting for properties of galaxies at optical and infrared wavelengths (see, for example, Kauffmann et al. 1993, Cole et al. 1994, Baugh, Cole & Frenk 1996, Kauffmann et al. 1999). The proposed disk formation mechanism should produce a signature at X-ray wavelengths which, in principle, is detectable with the present generation of satellites.

At the virial temperature of galaxy halos, the dominant cooling mechanism is X-ray Bremsstrahlung. If the cooling rate is significant, this flux may be visible as a component of diffuse X-ray emission extending well beyond the galaxy's optical radius. In this paper, we set out to test this disk formation model by looking for X-ray emission from the hy-

pothesized reservoir of cooling gas around three large, late-type galaxies, NGC 2841, NGC 4594 and NGC 5529.

If we assume that the mass of the present disk has been built up by a constant rate of accretion over the age of the universe (t_0), a simple estimate of the X-ray luminosity can be made from the binding energy of the disk.

$$L_X \approx \frac{\frac{1}{2} M_{\text{disk}} v_{\text{esc}}^2}{t_0} \quad (1)$$

where M_{disk} is the present mass of the disk, $v_{\text{esc}} = V_c [2 \ln(r_{\text{vir}}/r_{\text{disk}}) + 2]^{1/2}$ is the velocity required by material at the edge of the disk to escape the halo (assuming a flat rotation curve) and V_c is the measured circular velocity of the disk. Adopting parameters suitable for a large spiral galaxy such as NGC 2841 (ie., $M_{\text{disk}} = 5 \times 10^{10} M_{\odot}$, and $V_c = 317$ km/s), this suggests that the halo should emit a bolometric luminosity of at least $\sim 8 \times 10^{41}$ ergs s^{-1} *. If supernovae and other feedback processes are effective in

* Unless otherwise stated we have

heating halo gas then even more energy must be radiated to assemble the observed disk. Note that eqn. (1) predicts a minimum $L_X \propto V_c^5$, and that the temperature of the cooling gas should scale as the halo virial temperature, $T_X \propto V_c^2$. Thus, it is important to search for emission in the most massive systems available.

The picture of hierarchical galaxy formation developed by White & Frenk (1991, WF91; see also Kauffmann et al. 1993, Cole et al., 1994) predicts halo X-ray luminosities more directly by computing the cooling rate of gas as a function of time. At the present epoch, such models (which are tuned to reproduce the observed optical properties of galaxies) predict an X-ray luminosity of about 10×10^{41} ergs s^{-1} for galaxies like NGC 2841.

To date, studies of X-ray emission from nearby galaxies (e.g. Read, Ponman & Strickland, 1997) have concentrated on X-ray emission on scales comparable to the optical image of the galaxy. While extended emission has been detected in some groups of galaxies (e.g. Mulchaey et al. 1996, Trinchieri, Kim & Fabbiano 1994, Trinchieri, Fabbiano & Kim 1997), this emission is thought to be associated with the group potential. Our aim here is to test for the equivalent emission in *isolated* spiral galaxies, which we would identify with a cooling flow supplying the galaxy disk with gas. A few studies have reported diffuse emission from isolated elliptical galaxies. However, this has been interpreted either as resulting from the expulsion of gas from the galaxy (e.g. Read & Ponman 1998, Mathews & Brighenti 1998) or as a relic of a collapsed group (Ponman et al. 1994). Furthermore, since in hierarchical models of galaxy formation ellipticals are not necessarily expected to be accreting gas at the present day, the existence or otherwise of a diffuse X-ray component associated with them does not provide a strong test of such theories. For this reason, we have restricted our study to isolated spiral galaxies.

Previous X-ray observations of spirals (see, for example, Fabbiano & Juda 1997, Burstein et al. 1997, Pellegrini & Ciotti 1998, Brighenti & Matthews 1999) do not place strong constraints on the models we aim to test. These studies have focussed on measuring X-ray fluxes in regions comparable to the optical radius of the galaxy, where the intensity is strongest. X-ray emission from galactic stellar sources and uncertainties in the spatial X-ray surface brightness profile make it difficult to determine what fraction, if any, of the observed X-ray flux could be due to a low surface brightness cooling flow.

Since the cooling gas must, at some point, settle into the galaxy's disk, some emission is expected from this region as the gas cools from the virial temperature of the halo to much lower temperatures. For example, in the case of NGC 4594 models of the type considered here predict a luminosity comparable to that measured by Fabbiano & Juda (1997), $8.9 \pm 1.4 \times 10^{40}$ ergs/s in the 0.1-2.4keV band within the optical radius of the galaxy. However, likely contamination by stellar sources complicates the interpretation of this comparison.

In order to test the models in a manner free from uncertainties of the type just described it is essential to look for

low surface brightness emission at large distances from the optical disk of the galaxy. It is also necessary to study the optically brightest galaxies since the expected X-ray luminosity depends so strongly on the circular velocity of the galaxy's halo. For this reason, we have chosen for this study nearby galaxies with particularly high circular velocities. Most previous work has studied relatively low mass galaxies from which only relatively weak emission is predicted.

If diffuse X-ray emission from gas in the haloes of isolated spiral galaxies proves undetectable, this need not imply that the mass of halo gas is small since the gas may simply be too diffuse to emit X-rays efficiently. However, it would then be unable to cool and flow to the centre of the halo. We are thus testing whether the disks of spiral galaxies are being built up by the accretion of halo gas at the present day. The alternative is that spiral disks were assembled at higher redshift and evolved as essentially closed systems thereafter.

The structure of our paper is as follows. In §2, we search for large-scale diffuse emission from massive spiral galaxies. We are not able to make any convincing detection; the upper limits we establish are almost an order of magnitude below the predictions of the WF91 model. In §3 we discuss the uncertainties in the models and describe how they might be modified to agree with the data. The prospects for future investigations are outlined in §4.

2 OBSERVATIONS

2.1 Target Selection

The primary aim of this paper is to search for diffuse X-ray emission from nearby isolated spiral galaxies. The galaxy must be nearby for the signal to be detectable. Furthermore, the galaxy must have a high circular velocity in order that the energy released by the cooling gas be large. A high circular velocity also favours detectability because it implies a high characteristic temperature for the emission and so less absorption by neutral hydrogen in the Milky Way. In addition the efficiency of supernovae feedback is expected to decline with increasing circular velocity.

We created a suitable target list by searching for all spiral galaxies with recession velocities below 3000 km s^{-1} and with HI 20% line widths greater than 580 km s^{-1} . Of the sixteen galaxies satisfying these criteria three have been observed by the ROSAT PSPC: NGC 2841, NGC 4594 (the Sombrero galaxy) and NGC 5529. The PSPC data for these fields were obtained from the Leicester Database and Archive Service (LEDAS).

- NGC 2841. The Sb galaxy NGC 2841 is the nearest of our target galaxies. It has a flat rotation curve extending to the limit of HI observations, and is an archetype of galaxies with massive dark matter haloes (Kent, 1987). Its star formation properties have been studied extensively by Young et al. (1996) using both $H\alpha$ and far infra-red indicators.

- NGC 4594. Also known as M104 or the ‘‘Sombrero Galaxy,’’ this is a highly luminous Sa seen almost edge on. Since this galaxy is bulge dominated, diffuse X-ray emission similar to that seen around E or S0 galaxies (Forman, Jones & Tucker 1985) might be expected. However, X-ray observations by the *Einstein* satellite revealed spectral properties

assumed $H_0 = 50$ km s^{-1} Mpc $^{-1}$, $\Omega_0 = 1$, $\Lambda_0 = 0$, $\Omega_b = 0.06$ and $\sigma_8 = 0.67$

Table 1. Observed properties of the galaxies. Shown for each galaxy are its heliocentric radial velocity, distance, W_{20} (the width of the 21cm line at 20% of its peak intensity), N_{H} (the column density of neutral hydrogen in the Milky Way in the direction of the galaxy), r_{optical} (the 25 B-magnitudes per square arcsecond isophotal radius of each galaxy measured along the major axis), M_{B} (the absolute B-band magnitude) and morphological type.

Name	Heliocentric radial velocity (km/s) ^a	Distance (Mpc)	W_{20} (km s ⁻¹) ^d	N_{H} (10 ²⁰ cm ⁻²) ^e	r_{optical} (arcmin) ^d	M_{B}	Hubble type
NGC 2841	638 ± 3.0	13.8 ± 5.2 ^b	674 ± 4	1.45	4.1 ± 0.04	-20.6 ± 0.2	Sb
NGC 4594	1091 ± 5.1	24.54 ± 2.5 ^c	753 ± 7	3.67	4.4 ± 0.04	-23.0 ± 0.2	Sa
NGC 5529	2885 ± 5.1	57.72 ± 2.5 ^c	592 ± 5	1.09	3.3 ± 0.07	-21.1 ± 0.2	Sc

^a From the NASA Extragalactic Database (NED).

^b de Vaucoulers (1979)

^c From heliocentric radial velocity plus peculiar velocity correction assuming $H_0 = 50 \text{ km s}^{-1} \text{ Mpc}^{-1}$.

^d From the RC3 catalogue (available from NED), corrected for inclination.

^e Dickey & Lockman (1990).

Table 2. Measured rotation velocity and predicted gas temperature for the galaxies in our sample.

Name	V_c (km s ⁻¹) ^a	T_{vir} (keV) ^b
NGC 2841	317 ± 2	0.287 ± 0.004
NGC 4594	358 ± 4	0.366 ± 0.009
NGC 5529	277 ± 3	0.219 ± 0.005

^a Calculated from HI line widths using the expression given in Tully & Fouqué (1985)

^b As defined by White & Frenk (1991)

and core X-ray colours typical of less massive spiral galaxies (Kim, Fabbiano & Trinchieri 1992).

- NGC 5529. This is an Sc galaxy seen almost edge-on. Because of its relatively large distance, this galaxy is likely to provide weaker constraints than the previous two.

Distances, line widths, optical radii, and other relevant properties of these galaxies are listed in Table 1. The distances to two of them (NGC 4594 and NGC 5529) had to be determined from their observed heliocentric radial velocity; a model of the local peculiar velocity field (Branchini et al. 1999) was used to correct the observed velocity to the true Hubble velocity using an iterative procedure. Table 2 lists the circular velocity of each galaxy as calculated from its HI line-width and also the virial temperature of the halo estimated, as in WF91.

2.2 Data Reduction

Ideally, we would like to compare the X-ray flux from an annulus centered on the galaxy (but excluding the optically bright region to avoid contamination from stellar emission) with similar annuli centred on blank fields. This is not possible, however, because different ROSAT fields have different particle backgrounds. We have therefore adopted the procedure of first subtracting the detected events from a large radius annulus in the outer part of the PSPC detector as described in Snowden et al. (1994). Background corrected ‘on source’ and ‘off source’ fields may then be compared to determine the flux from the diffuse halo of the target galaxies.

It is important to note that the background subtraction algorithm of Snowden et al. tends to produce negative flux in the off-source images because of the different point-source detection thresholds in the centre and outer parts of the ROSAT field. Our analysis takes this effect into account.

The analysis of the data was carried out using the *As-terix* package. The procedure for analysing each image was as follows. Firstly, point sources were detected down to a 3σ threshold and excluded by cutting out a circle centred on each source. The radius of this circle was set equal to the radius of the PSF enclosing 95% of the energy at the position of each source. For each image a background annulus of inner radius 0.5° and outer radius 0.7° was then used to estimate the vignetting corrected background count-rate, and to create two background-subtracted spectra from source-centred annuli with inner radius of 5 arcminutes and outer radii of 9 and 18 arcminutes. Choosing a fixed angular radius ensures that the blank field analysis is the same for each image. The outer radius was chosen to include the entire inner ring of the PSPC. This is comparable to the predicted X-ray emitting region of the closer of our target galaxies (see §3). The $9'$ ring is matched to the X-ray emitting region of the more distant galaxy NGC 5529. The innermost aperture was excluded from the analysis in order to avoid contamination by the diffuse and unresolved stellar X-ray emission of the galaxy itself (cf. Read, et al. 1997, for example). The X-ray image of each galaxy is compared with the optical image in Figure 1.

The resulting spectra were analysed with the XSpec package to determine the source flux using the *mekal* X-ray emission and *wabs* absorption models. For each halo we adopted a virial temperature of 0.2keV. This is slightly below the virial temperatures estimated in Table 2, in order to obtain conservative estimates of the bolometric luminosity. The hot halo gas is assumed to have a metallicity of $0.3Z_\odot$ (where Z_\odot is the Solar metallicity). Neutral absorption column densities varied between the fields and were taken from Dickey & Lockman (1990). The only remaining free parameter in these models is the overall normalization. This procedure appropriately weights the contributions of the different energy channels and corrects for the different neutral hydrogen cross-sections of the fields.

The fitted spectrum is then used to calculate the ab-

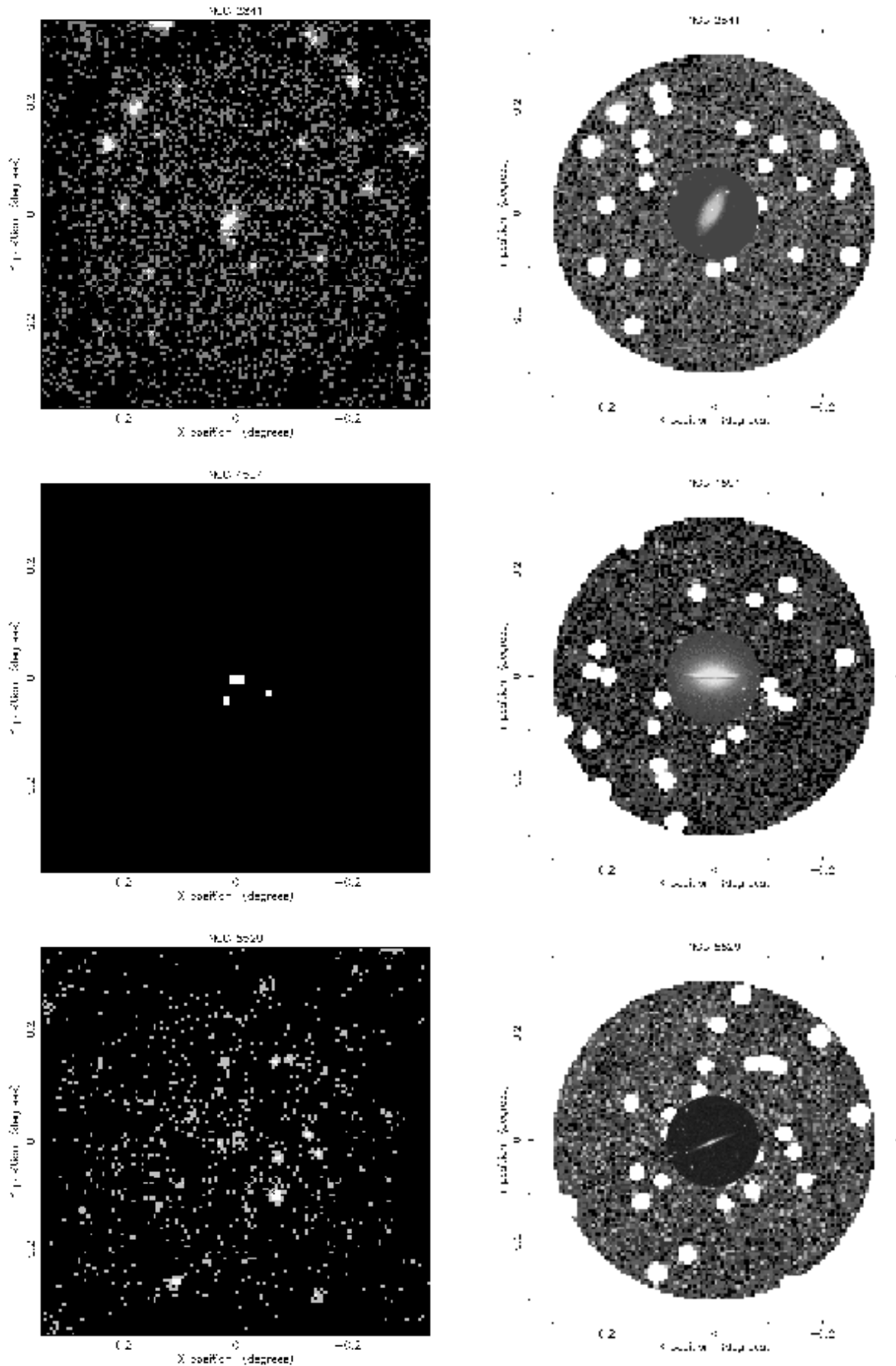


Figure 1. Source images for each galaxy in the sample. The left hand column shows the raw image @000 HzS, hMFBAS,000,100,000 after background subtraction, point source removal and selection of the region from 5 to 18 arcminutes. An optical image of each galaxy is superimposed on the X-ray image to give an appreciation of the size of the halo region.

Table 3. X-ray fluxes and bolometric luminosities for the haloes of three spiral galaxies. The fluxes and luminosities are determined for two annuli, with inner radius of 5 arcminutes and outer radii of 9 (ring 1) and 18 (ring 2) arcminutes. The first column gives the name of the galaxy. The flux corrected for blank field offsets is given in the following two columns, and the final two columns list the bolometric luminosity of each halo corrected for blank field offsets.

Galaxy	Bg. Corr.	Bg. Corr.	Bolometric	Bolometric
	Flux (ring 1) (10^{-14} ergs/cm ² /s)	Flux (ring 2) (10^{-14} ergs/cm ² /s)	L_X (ring 1) (10^{41} ergs/s)	L_X (ring 2) (10^{41} ergs/s)
NGC 2841	5.62 ± 10.33	22.90 ± 19.87	0.03 ± 0.06	0.16 ± 0.13
NGC 4594	17.96 ± 11.33	14.21 ± 22.40	0.44 ± 0.28	0.34 ± 0.54
NGC 5529	5.91 ± 10.03	-2.28 ± 19.22	0.78 ± 1.34	-0.29 ± 2.48

Table 4. The total counts per second in six blank fields. Background and point sources were removed in each case and an annulus from 5 to 9 arcminutes (ring 1) and from 5 to 18 arcminutes (ring 2) was selected.

Field	Ring1	Ring 2
rp201558	-0.017 ± 0.007	-0.063 ± 0.015
rp700255	-0.004 ± 0.006	-0.040 ± 0.013
rp700319	-0.021 ± 0.005	-0.024 ± 0.011
rp700376	-0.007 ± 0.005	-0.003 ± 0.011
rp700387	$+0.007 \pm 0.004$	-0.013 ± 0.008
rp700389	-0.005 ± 0.006	-0.023 ± 0.013

sorption corrected flux from each halo. These fluxes, shown in Table 3, are within the range 0.2 to 2.0 keV in order to minimise dependence on the assumed temperature. These are converted to pseudo-bolometric luminosities (0.001 to 10.0 keV) using the conservative temperature of 0.2 keV and the distances given in Table 1.

For comparison, six off-source fields (Table 4) with point source targets were selected at random from the ROSAT International X-ray/Optical Survey (RIXOS) (Mittaz et al. 1998). As we have previously noted, the analysis procedure tends to produce a small negative count-rate when applied to the off-source fields. This is due (at least in part) to the different flux limits at which point sources are removed from the target and background annuli. The mean luminosity deficit in the off-source fields was added to the measured luminosities of the target galaxies to correct for this effect. Alternatively one could add the off-source field count rates to the on-source fields and only then fit a model spectrum to the resulting counts to determine a corrected luminosity. We investigated performing the analysis in both ways and found that each procedure gives the same result to within 10%. Since the off-source count rates vary from field to field it is possible that the true correction required for each target field is somewhat different from the mean correction from the off-source fields. We therefore measure the variance in the off-source field correction and add this quantity in quadrature to the errors on the fluxes measured in our target fields. The variations from field to field are our dominant source of uncertainty.

The luminosities of the target galaxies are presented in Table 3. For each galaxy we expect a luminosity around 10×10^{41} ergs s⁻¹. However none of the galaxies is detected at a 3σ confidence level in either of the annuli considered. In-

stead, our data sets 95% upper confidence limits of 0.37, 1.2 and 3.8×10^{41} ergs s⁻¹ in the larger aperture for NGC 2841, 4594 and 5529 respectively. For NGC 5529, the relatively weak upper limit is due to the galaxy’s larger distance. For the two more nearby galaxies, the upper limit lies an order of magnitude below the initial theoretical prediction.

2.3 Uncertainties in the Observations

In §3, we consider possible modifications to the model of WF91 that might alleviate the discrepancy with our data. First, we take a closer look at the assumptions we made in interpreting the observational data. There are a number of uncertain quantities that could affect our conclusions. Throughout the analysis we have consistently assumed conservative values for these quantities (i.e. those that would minimize the conflict between model and data.) It is nevertheless instructive to consider how these choices might affect our results.

The dominant source of uncertainty in our analysis is the process of background subtraction. Although an accurate estimation of the background from a mosaic of surrounding pointings would be preferable, our off-source fields indicate the magnitude of the uncertainty. Even using the ‘worst case’ field (rp201558), the predicted and observed count-rates still disagree by a factor of 2–3.

Another important source of uncertainty is the extrapolation from ROSAT count-rate to bolometric flux. At the low temperatures appropriate to galactic halo gas, neutral hydrogen absorption in our own Galaxy has a strong effect. If our adopted values for the neutral hydrogen column density were inaccurate, this could have a substantial effect on our results. However these galaxies are at high Galactic latitude and we find that increasing the assumed column density by a factor of 3 over the values given by Dickey & Lockman (1990) only changes the inferred bolometric luminosity by 40%.

The effects of background correction and absorption alone cannot reconcile the observed and predicted luminosities. Altering the assumed temperature of the halo plasma, however, is a more promising alternative. This sensitivity arises because, at the relevant temperatures, most of the emission lies outside the 0.2–2.0 keV band of the observations, forcing us to extrapolate the model fit to lower energies. For example, at a temperature of 0.2 keV, 90% of the bolometric luminosity is emitted in the ROSAT 0.2–2.0 keV band, while at 0.1 keV, only 75% of the emission lies in this

band. At even lower temperatures, the effect becomes even more pronounced. Applying a lower temperature model to the observed spectra, we find that a decrease in temperature by a factor of 4.0 (for NGC 2841) to 4.5 (for NGC 4594) is required to bring the observations into line with the predicted luminosity. It is not clear, however, how these lower temperatures can be accommodated within the theoretical model. We now turn to a detailed examination of this model.

3 DISCUSSION

The model presented by WF91 predicts that the X-ray luminosity due to gas cooling within a dark matter halo should be:

$$L_X = \dot{M}_{\text{cool}}(r_{\text{cool}}) V_c^2 \ln \left(\frac{r_{\text{cool}}}{r_{\text{optical}}} \right), \quad (2)$$

where $\dot{M}_{\text{cool}}(r_{\text{cool}})$ is the rate at which mass is cooling in the dark matter halo, r_{cool} is the cooling radius (which grows with time), and r_{optical} is the optical radius of the galaxy, which we take to be the extent of the 25 B-magnitudes per square arcsecond isophote along the major axis. This model assumes that the halo has an isothermal potential with circular velocity V_c . As shown in the Appendix, the model can be readily extended to the case where the gravitational potential follows the functional form favoured by Navarro, Frenk & White (1996, NFW).

We have used the formulae and parameter choices in the Appendix to predict the bolometric X-ray luminosity for each of the three galaxies (using the circular velocities of Table 2), as well as the region in which cooling is expected to occur. Table 5 lists the cooling radii and luminosities of the haloes predicted by WF91's standard model and by a model with an NFW potential. In column 5, we list the luminosity that is expected within the 5-18' annulus used in the observational measurements. This geometric correction is made under the assumption of an isothermal flow in quasi-hydrostatic equilibrium as described in the Appendix. The figure given includes a correction for the flux from the target galaxy that is expected in the outer background annulus by extrapolating beyond the cooling radius with an r^{-2} density profile. The corrected flux is about 50% and 70% of the total for NGC 2841 and NGC 4594 respectively. The larger correction for NGC 2841 arises because the emission from the target almost fills the PSPC field of view. The geometric correction for NGC 5529 is greater because a large proportion of the luminosity is projected onto the optical image of the galaxy. In the case of this galaxy, the large observational uncertainties mean that the emission model is only weakly constrained.

For both NGC 2841 and NGC 4594 the bolometric X-ray luminosities predicted by the model are strongly inconsistent with the observations. The WF91 model predicts cooling rates of 7.4 and $9.0 M_{\odot} \text{yr}^{-1}$ for NGC 2841 and 4594 respectively. Since the mass cooling rate is proportional to the X-ray luminosity in these theories, the simplest interpretation is that the cooling rates in these galaxies are also much less than those predicted by WF91. If we assume that the geometric factors would be unchanged by reducing the cooling rate, we arrive at upper limits to the present-day accretion rate of 0.5 and $1.44 M_{\odot} \text{yr}^{-1}$.

Further insight can be gained by considering the total mass of gas within the cooling radius and the mass of the galaxy disk. In the case of NGC 2841 the disk mass can be determined by fitting the galaxy rotation curve. Kent (1987) derives a disk mass of $9.3 \times 10^{10} M_{\odot}$ allowing a free-fit of disk and isothermal halo parameters. Adopting an NFW model for the halo, Navarro (1998, N98) derives a best-fit disc mass of $5 \times 10^{10} M_{\odot}$; a significantly smaller disk mass would be inconsistent with the blue luminosity of the disk (Young et al., 1996). The WF91 model prediction for the mass of gas within r_{cool} , which is assumed to have formed the disk, is $9.8 \times 10^{10} M_{\odot}$. Thus the model allows enough gas to cool to make the observed disk. Consequently X-ray observations imply that the present-day accretion rate does not significantly contribute to the total disk mass. Clearly, this is an important result, since (if these galaxies are representative) it implies that the masses of spiral disks have remained almost constant over recent look-back times. Finally, we can compare the gas accretion rate with the star formation rate in NGC 2841 of $0.8 M_{\odot} \text{yr}^{-1}$ inferred from H α emission (Young et al. 1996). Thus, although our data exclude an infall rate sufficient to build the disk over a Hubble time, they may allow enough infall to replenish the gas being used up by star formation.

Before reaching wide-ranging conclusions, however, we must ask whether it is possible to modify the emission model to bring it more into line with the observational data. Below we consider possible modifications to the halo model that might reduce the discrepancy with the observational results.

Feedback. We have chosen galaxies with particularly deep potential wells in order to minimise the uncertainties arising from supernovae feedback effects on our predictions. According to the models of Kauffmann et al. (1993) and Cole et al. (1994) feedback in ~ 300 km/s halos reduces the predicted star formation rate by only $\sim 5\%$. Any gas ejected from the galaxy by feedback should begin cooling once more, and may actually increase the X-ray luminosity above our theoretical predictions. Feedback in these models cannot, therefore, reconcile theory and observations. However, in other models of galaxy formation, such as that of Nulsen & Fabian (1995, 1997) and Wu, Nulsen & Fabian (1999), in which feedback in earlier generations of dark matter halos alters the gas density profile (thereby reducing the cooling rate), the expected X-ray luminosities of spiral halos are likely to be substantially less than in the models we have tested. Although these models do reduce the luminosity of X-ray halos to levels consistent with our data, the cooling rate at late times appears much too small to allow the growth of disks as large and as massive as those observed. Further work is needed to investigate this point further.

Cosmological Parameters. The predicted X-ray luminosities have a relatively weak dependence on the values of the cosmological parameters (here we adopted $H_0 = 50 \text{ km s}^{-1} \text{Mpc}^{-1}$, $\Omega_0 = 1$, $\Lambda_0 = 0$, $\Omega_b = 0.06$ and $\sigma_8 = 0.67$). The strongest dependence is on the baryon fraction since the cooling rate is proportional to the square of the density of the X-ray emitting plasma. Using $\Omega_b = 0.04$ (a 50% reduction) reduces the luminosities by a factor ~ 2 , but at the expense of lowering the mass cooling rate also by a factor ~ 2 . Reasonable changes in cosmological parameters are unable to lower the predicted X-ray luminosity by

more than a factor ~ 3 . In particular, lowering Ω_0 tends to increase the cooling rate (and consequently the X-ray luminosity) because the baryon fraction of the halo is then increased.

X-ray Emission Temperature. An assumption of the model is that the X-ray emission occurs at a characteristic temperature close to that of the galactic halo. If the plasma had a multiphase structure, then the emission weighted temperature could be lower. However, a 25% decrease in temperature reduces the expected flux by only 20%. Much larger changes in temperature are required in order to account for the discrepancy.

Spatial Distribution of X-ray Emission. Because the cooling radius estimated for NGC 2841 is so large, the correction for the spatial distribution of the X-ray emission is important. In our standard model, approximately 60% of the total luminosity is emitted within the 5–18 arcminute annulus which we observe. If, for example, we considered a very different spatial distribution for the luminosity (whilst keeping the total luminosity the same), such as one in which the X-ray emissivity remains constant within the cooling radius, then the fraction of the total luminosity emitted within the annulus would drop to around 30%. The luminosity (corrected for geometric effects) listed in Table 5 would therefore be reduced by a factor of 2. These corrections are much less important for NGC 4594 where the cooling radius is better matched to the PSPC field of view.

Halo Circular Velocity. The luminosity of the flow is based on the premise that the high circular velocities of the disks of these galaxies reflect the circular velocities of the halo that confines the hot plasma. Recently, several authors (Zaritsky et al. 1997, N98) have suggested that high circular velocity galaxies could have formed in significantly cooler haloes. N98 has analyzed the rotation curve of NGC 2841, and found a best fitting model with $V_{200} = 167_{-13}^{+134}$ km s $^{-1}$ (where V_{200} is the circular velocity at the virial radius). Using the corresponding potential in the calculation of the X-ray luminosity we predict a substantially reduced X-ray emission of 0.9×10^{41} ergs s $^{-1}$ (including geometric factors), in much better agreement with the observational results. The ratio of the predicted value to the observational upper limit is 0.62. Unfortunately such a model underpredicts the disk mass inferred by N98 by a factor of 4. Increasing the gas fraction to remedy this problem restores the predicted X-ray luminosity to an unacceptably high value.

Metal abundance. We have assumed that the hot gas in the haloes has a metal abundance similar to that measured in galaxy clusters, namely $Z = 0.3Z_{\odot}$. Using $Z = 0.5Z_{\odot}$ increases the predicted X-ray luminosity by approximately 30%, since gas with a higher metal content can cool more efficiently. Reducing the abundance to $0.1Z_{\odot}$ would, for the same reason, reduce the predicted luminosities (and gas accretion rates), by a factor of ≈ 3 , but would also reduce disk masses by the same factor.

Remaining gas fraction. The predicted luminosity also depends upon the value of f_g , the fraction of the baryonic material in the halo that is in gaseous form at the time when the halo forms. This parameter is unlikely to be much less than the value of unity that we have assumed unless a significant fraction of the baryons in galaxies are in some dark form. Baugh et al. (1998) find that $f_g > 0.7$ for halos of circular velocity comparable to those of the galaxies considered

here. If f_g were lowered enough so that the predicted X-ray luminosity agreed with the observed upper limits, then the gas cooling rate would be significantly lower, making it impossible to build up a disk of the observed mass by the present. Therefore, although we do not know the exact value of f_g , a lower value cannot reconcile the model with both the observed X-ray luminosity and the inferred disk mass.

Multiphase flow. We have assumed that gas flows into the galaxy at the centre of the halo at a fixed temperature and only cools once it has settled in the galaxy disk. However, it is conceivable that the gas could instead cool “in-situ” (i.e. at the location in the dark matter halo where it originated) and then fall into the galaxy as cold clouds (Thomas, Nulsen & Fabian 1987). If this were indeed the case, then the bolometric X-ray luminosity emitted by the cooling gas would be $2.5\dot{M}_{\text{cool}}V_C^2$ (assuming that the gas cools at constant pressure). For typical values of r_{cool} and r_{optical} this is about half the luminosity predicted by eqn. (2). Furthermore, this luminosity would be emitted at a lower mean temperature than the virial temperature of the halo. Using the cooling flow model of Mushotzky & Szymkowiak (1988) we estimate that, for gas cooling from 0.2 keV, 11% of the bolometric luminosity would be emitted in the 0.2–2.0 keV band after accounting for absorption. This is approximately half of the 24% that is emitted in this band for gas at a fixed temperature of 0.2 keV. Thus, in the multiphase model the predicted flux in the 0.2–2.0 keV band is lower by a factor of approximately 4 compared to our standard model. These models are thus much less discrepant with the observational upper limits.

It should be noted, however, that even in this scenario the infalling gas must still release both its thermal and gravitational energy somewhere. The discussion above accounts only for the thermal component, and this model only succeeds if the gravitational component is radiated outside the ROSAT energy band. This not readily accomplished: if the cold clouds fall ballistically towards the centre, the gravitational energy would be radiated as post-shock X-rays when they collide with the galaxy’s gas disk. It does not help if the cold clouds are coupled to the hot gas by magnetic fields since although they could flow in more slowly by transferring their gravitational energy to the hot component, this energy will ultimately be radiated in the X-ray band.

Support for a multiphase model may be provided by the high-velocity clouds recently detected by Blitz et al. (1999) if these are indeed infalling onto the Milky Way. However, Blitz et al. estimate that the present day infall rate of such clouds onto the Milky Way is around $0.8M_{\odot} \text{ yr}^{-1}$, and this is significantly lower than the rate predicted by the models we consider ($\sim 5\text{--}6 M_{\odot} \text{ yr}^{-1}$). Thus, unless the observed clouds represent only a small fraction of the total cloud population, the simple multiphase model that we have considered seems to conflict with the inferred infall rate of cold gas onto the Milky Way.

4 CONCLUSIONS

We have searched for large-scale diffuse X-ray emission from three nearby, high rotation velocity spiral galaxies. In each case, we find that the observed emission is almost *an order of magnitude* below that required to build the disk at a

Table 5. Predictions from our models, assuming the standard cosmology and halo gas with $Z = 0.3Z_{\odot}$. Columns 3 and 4 list the total model luminosity and cooling radius in arcmin; column 5 gives the model luminosity after correction for the geometry of the source and background annuli; column 6 lists the ratio of the observed luminosity to the model luminosity after correction for the geometry.

Target	Halo model	Model $L_X/10^{41}$ ergs/s	R_{cool} (arcmin)	Geo. corrected Model $L_X/10^{41}$ ergs/s	Ratio of obs. 95% upper limit to model
NGC2841	Isothermal	10.4 ± 0.10	35.1 ± 13.7	5.5 ± 0.06	< 0.07
	NFW	7.6 ± 0.74	48.0 ± 18.1	4.5 ± 0.44	< 0.09
NGC4594	Isothermal	10.8 ± 0.18	18.7 ± 1.9	7.6 ± 0.13	< 0.16
	NFW	9.5 ± 0.63	23.0 ± 2.4	6.9 ± 0.46	< 0.17
NGC5529	Isothermal	3.4 ± 0.03	9.4 ± 0.4	1.3 ± 0.01	< 2.9
	NFW	2.4 ± 0.10	12.5 ± 0.5	0.9 ± 0.04	< 4.2

constant rate within the age of the universe. The accretion rate is similarly discordant with theoretical estimates of the cooling rate of gas in an isothermal or NFW-profile halo.

Although extremely suggestive, our results are not definitive. The reasons for this are:

- Strong constraints are derived only for the two nearer galaxies. We may, by chance, have selected two systems that have anomalous cooling rates. This is plausible for the bulge dominated NGC 4594 galaxy (‘the Sombrero’). NGC 2841 appears to be more typical of spiral galaxies, but its proximity makes accurate background subtraction difficult, and our results are dependent on the profile assumed for the X-ray emission. By contrast, the third galaxy meeting our selection criteria is too distant for strong limits on the X-ray flux to be set. We note, however, that the X-ray limits established for these galaxies are compatible with the emission that is thought to occur in the halo of our own galaxy (eg., Moore & Davis, 1994, Wolfire, et al. 1995).

- There are a number of parameters that have been assumed in order to predict the X-ray flux from the properties of the halo. No parameter, or combination of parameters, can simultaneously give a low X-ray luminosity and build the observed disk. To reconcile the predictions with the observed luminosities we must assume that either: (a) disks were built at high redshift; or, (b) accretion onto disks occurs without radiating the binding energy of the gas at X-ray wavelengths (e.g. in a multiphase flow).

Our results encourage further work. The current upper limits are set by our ability to subtract the background count-rate in the images. This is exacerbated in the ROSAT data because the flux level at which individual point sources may be subtracted varies across the image on scales comparable to the spiral galaxy haloes. Future work requires large-scale imaging with a detector that has a near-uniform detection threshold, such as the EPIC camera aboard the XMM satellite (Lumb et al. 1996). Such a survey would need to target a greater fraction of the nearby galaxies, setting firmer limits on the diffuse X-ray emission and eliminating variations in galaxy properties as a major source of uncertainty. If such work continues to fail to make detections, then we may be forced to conclude that spiral disks are no longer growing at the present epoch. This would agree with traditional models of galaxy formation in which galaxies accrete their mass at early times and evolve as more or less closed systems to the present-day. Clearly, there is much to learn from future studies of the X-ray haloes of spiral galaxies.

ACKNOWLEDGEMENTS

The authors would like to acknowledge Shaun Cole and Julio Navarro for providing rotation curve modelling code and best fit parameters for NGC 2841 respectively. We thank Enzo Branchini for making available to us his peculiar velocity field models prior to publication and Alan Smith for his work on a pilot version of this project as part of his undergraduate studies at the university of Durham. We have made use of the NASA Extragalactic Database (NED) and the Leicester Database and Archive Service (LEDAS). This project was carried out using computing facilities supplied by the Starlink Project, and was supported by a PPARC rolling grant for ‘Extragalactic Astronomy and Cosmology at Durham’ and by the European Community’s TMR Network for Galaxy Formation and Evolution. AJB and CSF acknowledge receipt of a PPARC Studentship and Senior Research Fellowship respectively. CSF also acknowledges a Leverhume Fellowship.

REFERENCES

- Abadi, M., Bower, R. G., Navarro, J., 1999, astro-ph/9904364 (submitted to MNRAS)
- Baugh C. M., Cole S., Frenk C. S., 1996, MNRAS, 283, 1361
- Baugh C. M., Cole S., Frenk C. S., Benson A. J., Lacey C. G., 1998, in P. Carral and J. Cepa eds., Star Formation in Early-Type Galaxies, ASP Conference Series, Vol. 163, Astron. Soc. Pac., San Francisco, p. 227.
- Bertschinger, E., 1989, ApJ, 340, 666
- Blitz L., Spergel D. N., Teuben P. J., Hartmann D., Burton W. B., 1999, ApJ, 514, 818
- Branchini E., Teodoro L., Frenk C. S., Schmoltd I., Efstathiou G., White S. D. M., Saunders W., Rowan-Robinson M., Keeble O., Tadros H., Maddox S., Oliver S., Sutherland W., 1999, MNRAS, 308, 1
- Brighenti F., Matthews H., 1999, AJ, 117, 1056
- Burstein D., Jones C., Forman W., Marston A. P., Marzke R. O., 1997, ApJS, 111, 163
- Cole, S., Lacey, C., 1993, MNRAS, 262, 627
- Cole S., Aragón-Salamanca A., Frenk C. S., Navarro J. F., Zepf S. E., 1994, MNRAS, 271, 781
- Cole S., Baugh C. M., Frenk C. S., Lacey C. G., 1999, in preparation
- de Vaucoulers G., 1979, ApJ, 227, 729
- Dickey J. M., Lockman F. J., 1990, ARAA, 28, 215
- Fabbiano G., Juda J. Z., 1997, ApJ, 476, 666
- Forman W., Jones C., Tucker W., 1985, ApJ, 293, 102

- Young, J. S., Allen, L., Kenny, J. D. P., Lesser, A., Rownd, B., 1996, *AJ*, 112, 1903
- Kauffmann G., White S. D. M., Guideroni B., 1993, *MNRAS*, 264, 201
- Kauffmann G., Colberg J. M., Diaferio A., White S. D. M., 1999, *MNRAS*, 303, 188
- Kent S. M., 1987, *AJ*, 93, 816
- Kim D.-W., Fabbiano G., Trinchieri G., 1992, *ApJS*, 80, 645
- Lumb, D., Eggel, K., Laine, R., Peacock, A., 1996, *Proceedings of the International Society for Optical Engineering (SPIE)*, 2808, 326
- Mittaz J. P. D., Carrera F. J., Romero-Colmenero E., Mason K. O., Hasinger G., McMahon R., Andernach H., Bower R., Burgos-Martin J., Gonzalez-Serrano J. I., Wonnacott D., 1999, *MNRAS*, 308, 233
- Mathews, W. G., Brighenti, F., 1998, *ApJ*, 503, 15
- Moore, B., Davis, M., 1994, *MNRAS*, 270, 209
- Mulchaey, J. S., Davis, D. S., Mushotzky, R., F., Burstein, D., 1996, *ApJ*, 456, 80
- Mushotzky R. F., Szymkowiak A. E., 1988, in "Cooling Flows in Clusters and Galaxies", ed. A. C. Fabian, Kluwer Academic Publishers, The Netherlands, p. 53.
- Navarro J. F., 1998, astro-ph/9807084 (submitted to *ApJ*) (N98)
- Navarro J. F., Frenk C. S., White S. D. M., 1996, *ApJ*, 462, 563 (NFW)
- Nulsen P. E. J., Fabian A. C., 1995, *MNRAS*, 277, 561
- Nulsen P. E. J., Fabian A. C., 1997, *MNRAS*, 291, 425
- Pelligrini S., Ciotti L., 1998, *A&A*, 333, 433
- Ponman T.J., Allan D. J., Jones L. R., Merrifield M., McHardy I. M., Lehto H. J., Luppino G. A., 1994, *Nature*, 369, 462
- Read, A. M., Ponman, T. J., 1998, *MNRAS*, 297, 143
- Read, A. M., Ponman, T. J., Strickland, D. K., 1997, *MNRAS*, 286, 626
- Snowden, S.L., McCammon, D., Burrows, D.N., Mendenhall, J.A., 1994, *ApJ*, 424, 714
- Thomas P. A., Nulsen P. E. J., Fabian A. C., 1987, *MNRAS*, 228, 973
- Trinchieri G., Kim D. W., Fabbiano G., 1994, *ApJ*, 428, 555
- Trinchieri G., Fabbiano G., Kim D. W., 1997, *A&A*, 318, 361
- Tully R. B., Fouqué P., 1985, *ApJS*, 58, 67
- White S. D. M., Frenk C. S., 1991, *ApJ*, 379, 52 (WF91)
- Wolfire, M. G., Mckee, C. F., Hollenbach, D., Tielens, A. G. G. M., 1995, *ApJ*, 453, 673
- Wu, K. K. S., Nulsen P. E. J., Fabian A. C., 1999, *MNRAS*, submitted.
- Zaritsky D., Smith R., Frenk C. S., White S. D. M., 1997, *ApJ*, 487, 39

APPENDIX A: A SIMPLE MODEL FOR THE X-RAY EMISSION FROM COOLING GAS

Following WF91, we assume that cooling occurs within a static potential, and that the cooling gas remains isothermal as it flows to the centre. The assumption of isothermality allows considerable simplification in the determination of the X-ray luminosity of the flow since it is directly related to the drop in potential energy (ie., the internal energy of the gas remains constant). Detailed, fully self-consistent flow models, such as those of Bertschinger (1989) and Abadi et al. (1999), show that these assumptions are reasonable over the range of scales over which we wish to determine the flow solution. The X-ray luminosity emitted by a unit mass of gas as it moves within the potential, ϕ , is

$$l_X = -v_R \frac{\partial \phi}{\partial r}. \quad (\text{A1})$$

In models such as those of Kauffmann et al. (1993) and Cole et al. (1994) gas is assumed to flow from the cooling radius towards the centre of the halo. No mass is assumed to fall out of the flow until it reaches the central galaxy. We find the total energy emitted by unit mass of gas as it flows inwards and then integrate from r_{cool} to r_{optical} to find the total energy emitted by the mass of gas,

$$q = \int_{r_{\text{optical}}}^{r_{\text{cool}}} -\frac{l_X(r)}{v_R(r)} dr. \quad (\text{A2})$$

If we now make the assumption that mass flows to the centre more quickly than the structure of the flow changes, then the structure of the flow at a snapshot in time can be represented by the trajectory of a single mass unit. Hence

$$L_X = \dot{M}_{\text{cool}}(r_{\text{cool}}) \int_{r_{\text{optical}}}^{r_{\text{cool}}} \frac{V_c^2(r)}{r} dr. \quad (\text{A3})$$

Below we consider two possibilities for the structure of the dark matter halo. In §A1 we consider an isothermal halo and in §A2 we consider the dark matter profile described by NFW, in each case assuming that the gas initially traces the dark matter.

A1 Cooling in an Isothermal Halo

This potential was considered by WF91. The dark matter density profile is $\rho(r) \propto r^{-2}$, where r is radial distance in the halo. The cooling radius, r_{cool} , in the halo is defined as the radius at which the cooling time, t_{cool} , of the gas equals the age of the Universe, t_0 . Ideally, we would use the time since the halo last doubled in mass (Cole & Lacey, 1993), but this information is not available for an individual galaxy. Since mass cooling rates decline with time, this leads to a conservative comparison with our observational results.

Assuming a spherically symmetric halo in which the gas is initially distributed like the dark matter, the cooling time is given by

$$t_{\text{cool}}(r) = \frac{192\pi\Omega_0 G m_p^2 r^2}{49 f_g \Omega_b \Lambda (\mu m_p V_c^2 / 2k)}, \quad (\text{A4})$$

(White & Frenk 1991), where Ω_b is the baryon fraction, $\Lambda(T)$ is the cooling function of the gas, f_g is the fraction of the initial baryon density remaining in gaseous form (which we normally assume to be 1), G is the gravitational constant, m_p is the mass of a proton, μ is the mean molecular weight of the gas, V_c is the circular velocity of the halo and k is Boltzmann's constant.

The evolution of the cooling radius determines the mass of gas cooling per unit time.

$$\dot{M}_{\text{cool}}(r_{\text{cool}}) = \frac{1}{2} \frac{f_g \Omega_b}{\Omega_0} \frac{V_c^2(r_{\text{cool}}) r_{\text{cool}} (V_{c,\text{max}}, z)}{G t_0}. \quad (\text{A5})$$

This can be combined with equation (A3) to estimate the total X-ray luminosity of the halo.

A2 Cooling in an NFW Halo

NFW provide a fitting formula for the density profiles of dark matter haloes in N-body simulations of hierarchical

clustering. This profile is characterised by two parameters: δ_c , a characteristic density, and r_s , a characteristic radial scale in the halo. NFW find that δ_c and r_s are correlated in any given cosmology so that the NFW profile provides a universal, one-parameter model of the halo. This formula provides a good approximation to the density profile of haloes of all masses over at least two orders of magnitude in radius and its shape is independent of the values of the cosmological parameters.

Appropriate parameters for the galaxy haloes in any given cosmology are determined by requiring that the measured circular velocity of the galaxy corresponds to the maximum in the NFW rotation curve. This must be fitted in an iterative fashion since the ratio between $V_{c,\text{vir}}$ and $V_{c,\text{max}}$ itself depends on $c = r_{200}/r_s$.

Using the circular velocity profile of an NFW halo, the cooling radius is defined by the relation

$$t_0 = \frac{192\pi}{49} \frac{1}{f_g} \frac{\Omega_0}{\Omega_b} \frac{Gm_p^2 r_s^2}{\Lambda(T_{\text{vir}})} \frac{x_{\text{cool}}}{x_{\text{vir}}} (1 + cx_{\text{cool}})^2 \times [\ln(1 + cx_{\text{vir}}) - cx_{\text{vir}}/(1 + cx_{\text{vir}})]^{-1}. \quad (\text{A6})$$

where $x = r/r_{200}$. We then obtain,

$$L_X = \dot{M}_{\text{cool}}(r_{\text{cool}}) V_c^2(r_{200}) \times \int_{x_{\text{optical}}}^{x_{\text{cool}}} x^{-2} \frac{\ln(1 + cx) - cx/(1 + cx)}{\ln(1 + c) - c/(1 + c)} dx, \quad (\text{A7})$$

where $x_{\text{cool}} = r_{\text{cool}}/r_{200}$ and $x_{\text{optical}} = r_{\text{optical}}/r_{200}$. This equation must be integrated numerically for any given c .